




# Death and survival of gut CD4 T cells following HIV-1 infection ex vivo

Kaylee L. Mickens <sup>a,b</sup>, Stephanie M. Dillon <sup>a</sup>, Kejun Guo <sup>a</sup>, Ashley N. Thompson <sup>a,b</sup>, Bradley S. Barrett<sup>a</sup>, Cheyret Wood <sup>c</sup>, Katerina Kechris <sup>c</sup>, Mario L. Santiago <sup>a,b,\*</sup> and Cara C. Wilson <sup>a,b,\*</sup>

<sup>a</sup>Division of Infectious Diseases, Department of Medicine, University of Colorado School of Medicine, 12700 E 19th Ave, Mail Stop B168, Aurora, CO 80045, USA

<sup>b</sup>Department of Immunology and Microbiology, University of Colorado School of Medicine, 12800 E 19th Avenue, Mail Stop 8333, Aurora, CO 80045, USA

<sup>c</sup>Department of Biostatistics and Informatics, Center for Innovative Design and Analysis, 13001 E 17th Place, Mail Stop B119, University of Colorado School of Medicine, Aurora, CO 80045, USA

\*To whom correspondence should be addressed: Email: [mario.santiago@cuanschutz.edu](mailto:mario.santiago@cuanschutz.edu); [cara.wilson@cuanschutz.edu](mailto:cara.wilson@cuanschutz.edu)

Edited By Carlos del Rio

## Abstract

The gastrointestinal tract is ground zero for the massive and sustained CD4 T cell depletion during acute HIV-1 infection. To date, the molecular mechanisms governing this fundamental pathogenic process remain unclear. HIV-1 infection in the gastrointestinal tract is associated with chronic inflammation due to a disrupted epithelial barrier that results in microbial translocation. Here, we utilized the lamina propria aggregate culture model to demonstrate that the profound induction of granzyme B by bacteria in primary gut CD4 T cells ex vivo significantly contributes to HIV-1-mediated CD4 T cell death. Counterintuitively, a substantial fraction of gut granzyme B+ CD4 T cells harboring high levels of HIV-1 infection survive via a pathway linked to CD120b/TNFR2. Our findings underscore previously undescribed mechanisms governing the death and survival of gut CD4 T cells during HIV-1 infection that could inform strategies to counter HIV-1 pathogenesis and persistence in this critical tissue compartment.

**Keywords:** HIV-1, cytotoxic CD4+ T lymphocytes, granzyme B, TNF response, gut immunology

## Significance Statement

HIV-1 causes AIDS by decimating CD4 T cells that are critical for immunity against pathogens. Notably, the CD4 T cells in the gut are more vulnerable to killing by HIV-1, resulting in the leakage of bacteria that was linked to debilitating chronic illnesses. The reason for the massive loss of CD4 T cells in the gut is not fully understood. Here, we show that bacteria drive the expression of a cytotoxic protein, granzyme B (GZB), in gut CD4 T cells, and the activity of GZB in gut CD4 T cells allows HIV-1 to effectively kill these critical immune cells. Interestingly, some GZB+ CD4 T cells survive HIV-1 infection via a mechanism linked to TNFR2. These findings may inform cure strategies aimed at the persistent HIV-1 reservoir in the gut.

## Introduction

CD4 T cells are the main cellular targets of HIV-1, and the preferential depletion of these cells is the hallmark of progression to AIDS (1). However, CD4 T cell depletion is not uniform across tissue compartments, as early in HIV-1 infection, CD4 T cells in the gastrointestinal (GI) tract are massively depleted, much more so than their counterparts in peripheral blood (2). Whereas peripheral blood CD4 T cell counts will recover after antiretroviral therapy (ART), gut CD4 T cells remain depleted in persons with HIV-1 (PWH) even after decades of ART (2). To date, the mechanisms driving gut CD4 T cell depletion remain unclear, as most studies on HIV-1-mediated CD4 T cell death have focused on CD4 T cell lines or mitogen-activated blood CD4 T cells infected with lab-adapted strains of HIV-1 that utilize CXCR4. Previous studies

using the human lymphoid aggregate culture (HLAC) model revealed that HIV-1 kills CD4 T cells via pyroptosis, an inflammatory form of death linked to caspase-1 (3). The CD4 T cells in the HLAC model were derived from tonsil tissue; therefore, the CD4 T cells investigated consisted mostly of central memory, follicular, and naive subsets, with only a small fraction (follicular regulatory cells) expressing CCR5 (4). By contrast, gut CD4 T cells consist mainly of tissue-resident effector memory subsets that express high levels of CCR5 and  $\alpha 4\beta 7$  (5). More recently, humanized mice (CD34+ cord blood model) were used to demonstrate that CARD8 sensing of HIV-1 protease leads to pyroptotic death of CD4 T cells (6). However, CD34+ cells show limited reconstitution in the gut of humanized mice (7). Thus, understanding the mechanism for how HIV-1 kills gut CD4 T cells may require ex vivo models that

**Competing Interest:** The authors declare no competing interests.

**Received:** September 17, 2024. **Accepted:** October 9, 2024

© The Author(s) 2024. Published by Oxford University Press on behalf of National Academy of Sciences. This is an Open Access article distributed under the terms of the Creative Commons Attribution-NonCommercial-NoDerivs licence (<https://creativecommons.org/licenses/by-nc-nd/4.0/>), which permits non-commercial reproduction and distribution of the work, in any medium, provided the original work is not altered or transformed in any way, and that the work is properly cited. For commercial re-use, please contact reprints@oup.com for reprints and translation rights for reprints. All other permissions can be obtained through our RightsLink service via the Permissions link on the article page on our site—for further information please contact journals.permissions@oup.com.

incorporate unique cellular targets obtained directly from the human GI tract.

A major feature of HIV-1 infection in the GI tract is the involvement of the microbiota; it is estimated that  $3.8 \times 10^{13}$  bacteria reside in the intestinal lumen (8). During acute HIV-1 infection, the loss of T helper (Th)17 cells in the gut contributes to the dysregulation of the epithelial barrier, resulting in the translocation of enteric commensal bacteria from the gut lumen to the underlying lamina propria and systemic circulation (9, 10). Microbial translocation leads to chronic immune activation and inflammation that increase the risk of cardiovascular disease, lung disease, kidney disease, liver disease, diabetes, and neurocognitive disorders among PWH even under ART (11, 12). To model the interactions between clinical HIV-1 strains, primary lamina propria mononuclear cells (LPMCs), and the microbiota *ex vivo*, we developed the lamina propria aggregate culture (LPAC) model (13–15). Using the LPAC model, we demonstrated that HIV-1 strains that utilize CCR5, including clinically relevant transmitted/founder (TF) HIV-1 strains, rigorously replicated and depleted gut CD4 T cells *ex vivo* (16–18). Exposure of LPMCs to diverse enteric bacteria enhanced HIV-1 replication (19), and CD4 T cell death could be blocked using a caspase-3, but not a caspase-1 inhibitor (14). These findings suggested that bacterial exposure augmented and shifted the mechanism of HIV-1-mediated gut CD4 T cell death from pyroptosis to apoptosis. These findings inform, but do not sufficiently explain, why gut CD4 T cells are much more susceptible to HIV-1-mediated killing.

To investigate molecular features of HIV-1 infection of gut CD4 T cells exposed to bacteria, we performed an unbiased transcriptomics study. We reported that genes altered following HIV-1 infection of gut CD4 T cells were fundamentally different from that of mitogen-activated blood CD4 T cells (17). Unexpectedly, microbial exposure and HIV-1 infection of gut CD4 T cells rapidly induced high levels of granzyme B (GZB) (16, 17), a serine protease mainly associated with the cytotoxic functions of CD8 T cells and natural killer (NK) cells (20). These data were confirmed at the protein level by flow cytometry (16). Notably, GZB induction barely occurred in peripheral blood or not at all in tonsil CD4 T cells, indicating that GZB induction due to bacterial exposure is a fundamental distinction between blood/tonsil versus gut CD4 T cells (16). A subset of gut GZB+ CD4 T cells co-expressed Granzyme A (GZA), perforin (a pore-forming protein), and/or CD107a (a degranulation marker), suggesting that gut CD4 T cells exposed to microbes  $\pm$  HIV-1 are primed to become CD4 cytotoxic T lymphocytes (CD4 CTLs) (16). Of note, many studies have demonstrated that GZB induces apoptosis when delivered into target cells (20). Since our studies in the LPAC model with microbial exposure linked apoptosis with HIV-1-mediated CD4 T cell death (14), in the first part of this study, we tested whether GZB directly participates in HIV-1-mediated killing of bacteria-exposed gut CD4 T cells.

Deciphering the mechanisms driving HIV-1-mediated CD4 T cell death is critical for a deeper understanding of HIV-1 immunopathogenesis. However, as the HIV-1 pandemic continues without an effective cure, unraveling the mechanisms driving persistence has also become important (21). Despite high levels of total CD4 T cell depletion, histological analysis of colon biopsies of untreated PWH revealed higher frequencies of GZB+ CD4 T cells compared with age-/sex-matched controls (16). This suggested that a subset of GZB+ CD4 T cells somehow survive HIV-1 infection *in vivo*. Notably, a recent single-cell transcriptomic (scRNAseq) study discovered that a substantial fraction of HIV-1 RNA+ CD4 T cells from peripheral blood of PWH under ART expressed GZB (22). This was corroborated by another study showing that the highest

frequency of HIV-1 RNA+ blood CD4 T cells by scRNAseq expressed cytotoxicity genes, including GZB (23). This raised the possibility that HIV-1 may persist in CD4 CTLs *in vivo* and serve as a potential reservoir. In the second part of this study, we thus also analyzed the GZB+ CD4 T cells that survive HIV-1-mediated depletion in the LPAC model *in vitro*. Altogether, our findings highlight plausible mechanisms for why HIV-1 is particularly adept at depleting CD4 T cells in the gut and raise novel insights on how HIV-1 could persist in mucosal compartments in the context of microbial translocation and inflammation.

## Results

### GZB+ CD4 T cells are preferentially infected with HIV-1 in the LPAC model

Exposure to diverse enteric bacteria enhanced HIV-1 replication and CD4 T cell depletion in the LPAC model (19). Given that bacteria also promoted GZB expression in CD4 T cells, we first compared HIV-1 infection levels in GZB+ and GZB– CD4 T cells and HIV-1-mediated depletion of these subsets. LPMCs ( $n = 8$  donors) were spinoculated with TF HIV-1 (CH040) (24) or mock for 2 h and then cultured for 4 days in the presence or absence of bacterial lysate (*Escherichia coli*) (Fig. 1A). At 4 days post-infection (dpi), LPMCs were collected and stained for flow cytometric analysis (Fig. 1B). Because HIV-1 downregulates CD4, viable infected CD4 T cells were gated as viable (AqVi–) CD3+ CD8– p24+. Consistent with our previous results, bacterial exposure increased HIV-1 infection from an average of 4.0 to 17.6% (Fig. 1C, Left). These results were reproduced using an eGFP-tagged version of the virus (Fig. S1A). Furthermore, bacterial exposure increased GZB expression in conditions with or without HIV-1 infection (Fig. 1C, Right). Productively infected (p24+) CD4 T cells more frequently expressed GZB than bystander (p24–) cells in the presence of bacteria (Fig. S1B), mirroring our previous data in LPMCs exposed to *Prevotella stercorea* (17) instead of *E. coli* lysate. Among cultures exposed to bacteria, GZB+ cells harbored 1.5-fold higher HIV-1-infected cells compared with GZB– cells (Fig. 1D). Thus, gut GZB+ CD4 T cells exhibited higher levels of HIV-1 infection in the LPAC model. Previously, we reported that commensal enteric bacteria increased the expression of CCR5 and markers associated with T cell activation (HLA-DR/CD38), which could explain why bacteria-stimulated gut CD4 T cells supported higher levels of HIV-1 infection (16). Notably, GZB+ CD4 T cells exhibited enhanced CCR5 expression (Fig. S1C) and T cell activation (Fig. S1D) relative to GZB– counterparts. We next evaluated the levels of CD4 T cell depletion. At 4 dpi, CD4 T cell depletion relative to mock-infected cultures averaged 43.3% (Fig. S1E). Both GZB+ and GZB– CD4 T cells were similarly depleted following HIV-1 infection (Fig. 1E). As GZB– CD4 T cells had significantly lower HIV-1 infection levels (Fig. 1D), these findings imply that substantial death was occurring among “bystander” (HIV-1-uninfected or abortively infected) CD4 T cells.

### HIV-1 infection of GZB+ CD4 T cells is associated with apoptosis

We previously demonstrated using caspase inhibitors that in the presence of bacteria, there was a shift in HIV-1-mediated CD4 T cell death from pyroptosis to apoptosis (14). GZB promotes apoptosis via the cleavage of multiple cellular targets, including procaspase-3 and Bid (20). We thus tested whether GZB expression in CD4 T cells is associated with apoptosis. LPMCs ( $n = 6$  donors) were spinoculated with TF HIV-1 (CH040) and cultured in the presence of *E. coli* lysate for 4 days. Viable (AqVi–) cells expressing Annexin V were tracked as cells at the early stages of

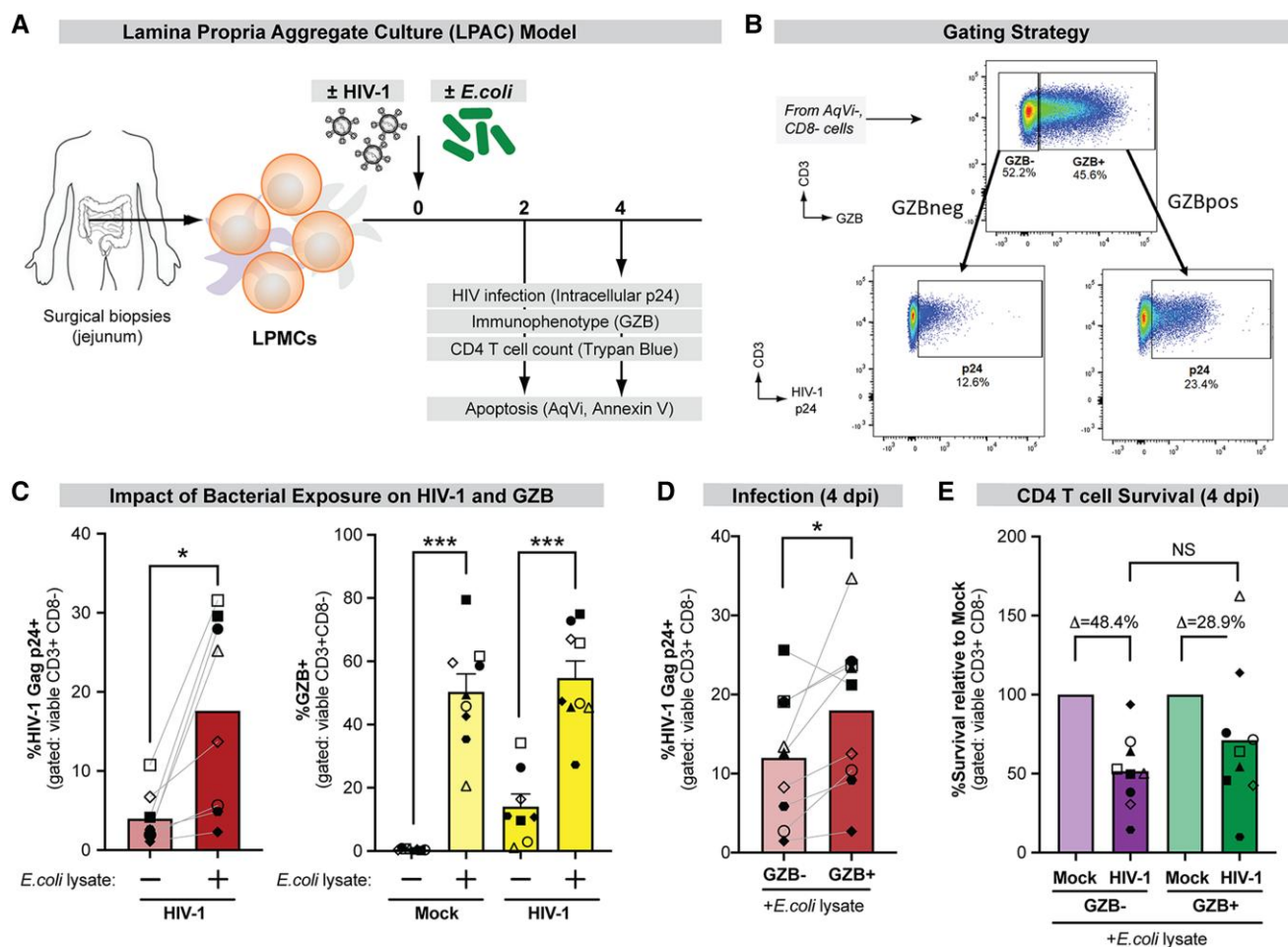


**Fig. 1.** HIV-1 infection and survival of GZB+ CD4 T cells in the LPAC model. A) Infection time course. At 0 dpi, LPMCs are spinoculated with TF HIV-1 for 2 h and then immediately cultured with commensal *E. coli* lysate. At 2 and 4 dpi, HIV-1 infection and viable CD4 T cell counts are measured. B) Gating strategy for GZB+ and GZB<sup>neg</sup> cells. Note that CD4 T cells were determined from CD3+ CD8- cells. C) Up-regulation of (Left) HIV-1-infected CD4 T cells ( $n = 9$  donors; paired t test) and (Right) GZB ( $n = 8$  donors for mock,  $n = 9$  donors for HIV-1-infected; mixed-effects model) following *E. coli* stimulation. D) HIV-1 infection in GZB+ versus GZB- CD4 T cells, based on the gating strategy in Fig. 1B ( $n = 9$  donors; two-tailed paired t test). E) Survival of GZB+ versus GZB- CD4 T cells following HIV-1 infection ( $n = 9$  donors; one-way ANOVA with Sidak's multiple comparisons test) in the presence of *E. coli* lysate.  $\Delta$  corresponds to the average CD4 T cell depletion relative to mock. CD4 T cell counts were normalized to mock-infected cultures as 100% for each donor. For each of C to E, each shape corresponds to a distinct LPMC donor. Bars represent mean ( $\pm$  SEM); \* $P < 0.05$ , \*\*\* $P < 0.001$ . ns, not significant.

apoptotic cell death (Fig. 2A and C). Given substantial CD4 T cell depletion at 4 dpi (Fig. S1E), we also evaluated apoptotic markers earlier at 2 dpi ( $n = 5$  donors). At both time points, total GZB+ CD4 T cells were more apoptotic than GZB- counterparts (Fig. 2B). A significantly higher frequency of apoptotic CD4 T cells were also detected in HIV-1-infected (p24+) versus uninfected (p24-) CD4 T cells (Fig. 2D). In addition, productively infected (p24+) GZB+ CD4 T cells are more frequently undergoing early apoptosis than bystander (p24-) GZB+ CD4 T cells (Fig. S1F). Altogether, these findings formally link HIV-1 infection of GZB+ CD4 T cells with apoptosis in the LPAC model.

### CD4 T cell-intrinsic GZB promotes CD4 T cell death following HIV-1 infection

The link between HIV-1 infection of GZB+ CD4 T cells and apoptosis, and our previous data showing that HIV-1-mediated killing of microbe-exposed gut CD4 T cells occurs via apoptosis, suggested that GZB may be a direct mediator of HIV-1-mediated killing. GZB serine protease activity can be blocked using Z-AAD-CMK (Enzo Biosciences), a cell-permeable peptide inhibitor based on the Ile-Glu-Pro-Asp (IEPD) cleavage site of GZB (25). LPMCs ( $n = 6$

donors) were infected with TF HIV-1 (CH040) or mock then exposed to bacterial lysate (*E. coli*) in the presence/absence of Z-AAD-CMK. On average, Z-AAD-CMK treatment blocked GZB activity by 64.2% (range: 40.1–100%) (Fig. 3A).

We next quantified HIV-1-mediated CD4 T cell death in the presence or absence of Z-AAD-CMK. Absolute CD4 T cell counts were calculated relative to mock controls for each donor by flow cytometry and automated cell counting (3, 13, 14). TF HIV-1 in the presence of *E. coli* lysate infection led to substantial CD4 T cell death: 43.4% of CD4 T cells died in HIV-1-infected cultures compared with mock (Fig. 3B). Notably, partial blockade of GZB activity (Fig. 3A) significantly rescued CD4 T cells from HIV-1-mediated death, with only 18.0% depleted with the GZB inhibitor (Fig. 3B). These data formally link GZB activity to HIV-1 mediated CD4 T cell killing in the LPAC model.

The LPAC model includes multiple immune cell types. While the majority of lymphocytes are CD4 T cells (64%), there is also a substantial fraction (20%) of CD8 T cells (13), one of the canonical producers of GZB. Gut CD8 T cells produce both GZB and perforin in culture over the time course of 4 days in response to *E. coli* lysate (Fig. S2). To confirm that GZB from CD8 T cells was not responsible for the effect of GZB on HIV-1-mediated CD4 T cell

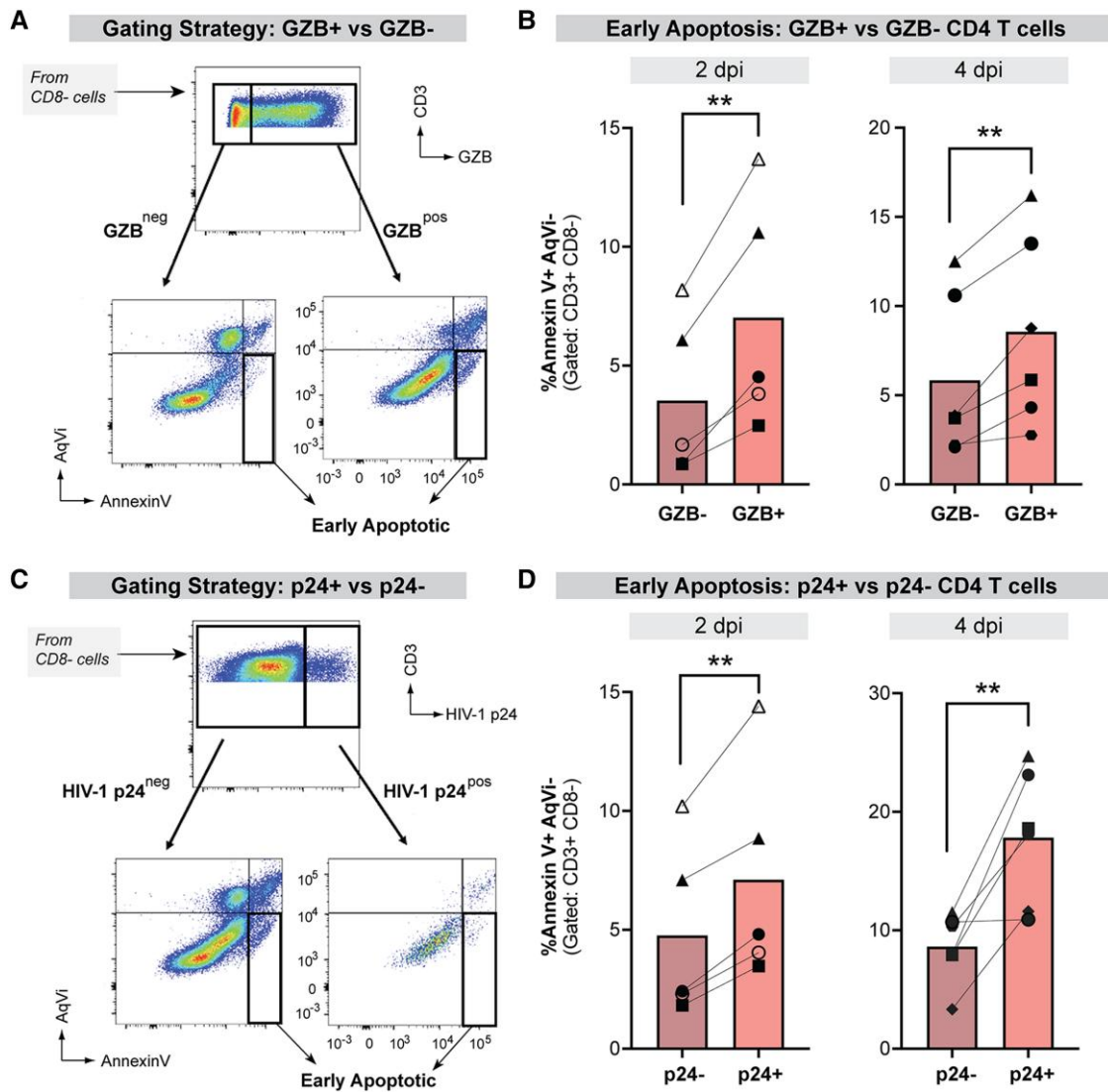


**Fig. 2.** HIV-1 infection and GZB expression are associated with apoptosis. LPMCs were spinoculated with TF HIV-1 or mock infected and cultured with commensal *E. coli* lysate for 2 or 4 days. A) Gating strategy. Early apoptotic cells are defined as viable (Aqua Viability dye negative) and Annexin V positive. B) Percentages of early apoptotic GZB+ or GZB- CD3+ CD8- T cells CD3+ CD8- T cells at 2 dpi ( $n = 6$ ) and 4 dpi ( $n = 5$ ). C) Gating strategy for early apoptotic HIV-1-infected (p24+) or uninfected (p24-) CD4 T cells. D) Percentages of early apoptotic infected or bystander CD3+ CD8- T cells at 2 dpi ( $n = 6$ ) and 4 dpi ( $n = 5$ ). Statistical analyses for B and D were performed using two-tailed paired t test. \*\* $P < 0.01$ .

death, we depleted LPMCs ( $n = 4$  donors) of CD8 T cells by magnetic cell separation. We then compared CD4 T cell survival between donor-matched total LPMC and CD8-depleted conditions at 4 dpi in the presence of *E. coli* lysate. On average, 89.6% of CD8 T cells were removed at 0 dpi (Fig. 3C). We did not observe a significant difference in HIV-1 infection (Fig. 3D) and intracellular GZB activity (Fig. 3E) in the presence or absence of CD8+ cells. At 4 dpi, the mean CD4 T cell survival in total LPMCs was 52.3%. Without CD8 T cells, CD4 T cell survival was slightly worse at 42.6%, indicating that the presence of CD8 T cells is not required for HIV-1 CD4 T cell death in the LPAC model (Fig. 3F). Thus, CD8 T cells do not contribute to CD4 T cell death in the LPAC model, and the GZB activity responsible for HIV-1-mediated CD4 T cell death was likely intrinsic to CD4 T cells (Fig. 3G).

### A subset of GZB+ CD4 T cells express biomarkers of cell survival

GZB activity is associated with HIV-1-mediated killing of gut CD4 T cells in the LPAC model (Fig. 3B), but GZB+ CD4 T cells are

readily detected during chronic HIV-1 infection in the gut in vivo, in higher frequency and number compared with gut tissue of people without HIV-1 (16). GZB+ CD4 T cells had higher levels of HIV-1 infection, but this did not translate to higher levels of depletion compared with GZB- CD4 T cells (Fig. 1E). We thus hypothesized that a subset of gut GZB+ CD4 T cells may have attributes that allow for survival following HIV-1 infection. To determine whether gut GZB+ CD4 T cells are heterogeneous, we performed unbiased single-cell transcriptomics (scRNAseq). Total LPMCs ( $n = 6$  donors) were cultured in the presence of *E. coli* lysate for 48 h, and then, CD4 T cells were isolated by magnetic and fluorescent cell sorting for the generation of V3 Chromium Single Cell 3' Transcriptome libraries. Altogether, we captured 48,934 CD4 T cells, of which 15,317 (31%) were GZB+ (Fig. 4A). Using the DICE T cell subset profiling pipeline (26), the majority of the GZB+ CD4 T cells following bacterial stimulation were categorized as Th1 (54.7%) and Th1/17 (27.1%), consistent with our previously published flow cytometry data (16), followed by Tregs (16%) (Fig. 4B).

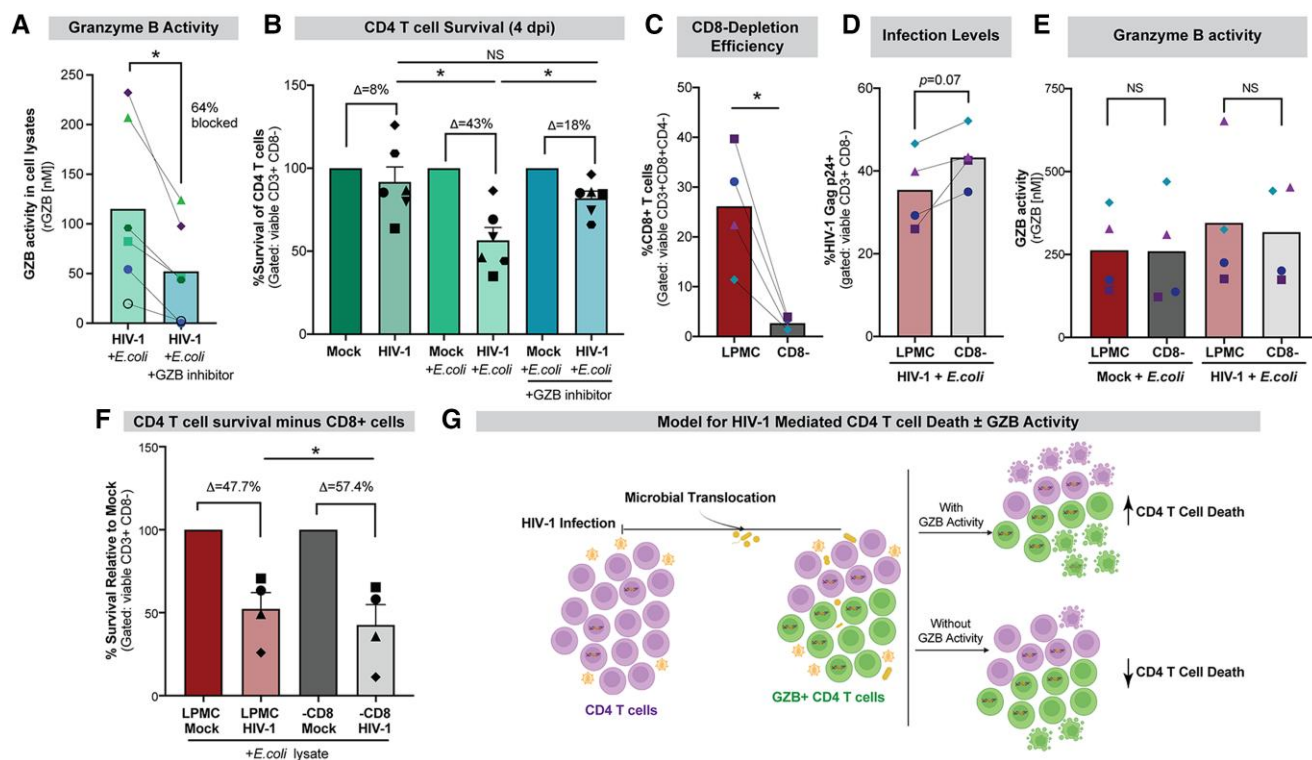


**Fig. 3.** Effect of CD4 T cell-intrinsic GZB on HIV-1-mediated CD4 T cell death. A), B) LPMCs were spinoculated with TF HIV-1 or mock and cultured with or without commensal *E. coli* lysate in the presence/absence of the GZB inhibitor Z-AAD-CMK (250  $\mu$ M) for 4 days. A) Intracellular GZB activity in cell lysates ( $n = 6$  donors; two-tailed paired t test) was determined using a colorimetric assay. GZB cleavage of Ac-IEPD-pNA releases pNA, which can be detected at 405 nm. B) Total CD4 T cell survival normalized to donor-matched mock infection ( $n = 6$  donors; Repeated Measures (RM) one-way ANOVA with Sidak's multiple comparisons test). C) LPMCs depleted of CD8 cells (–CD8) using magnetic beads were confirmed by flow cytometry ( $n = 4$  donors, two-tailed paired t test). D) to F) Total or CD8-depleted LPMCs were spinoculated with TF HIV-1 or mock then cultured with *E. coli* lysate for 4 days. D) HIV-1 infection levels in LPMC versus CD8-depleted LPMCs ( $n = 4$  donors, two-tailed paired t test). E) Intracellular GZB activity in cell lysates measured as in A. F) Total CD4 T cell survival normalized to matched mock control ( $n = 4$  donors, RM one-way ANOVA with Sidak's multiple comparisons test). For A to F, bars correspond to mean values;  $P < 0.05$ , NS, not significant;  $P$ -values  $< 0.1$  were noted. G) Model of HIV-1-mediated CD4 T cell death  $\pm$  GZB activity (Biorender.com). Microbial translocation up-regulates GZB in gut CD4 T cells. When GZB activity is present, more HIV-1-mediated CD4 T cell death occurs for both infected and bystander CD4 T cells (blebbing cells). When GZB activity is blocked, less HIV-1-mediated CD4 T cell death occurs, leaving a larger surviving population of CD4 T cells.

We identified 58 genes that were up-regulated  $> 1.5$ -fold and three genes that were down-regulated  $> 1.5$ -fold in GZB+ versus GZB– cells (Fig. 4C and Table S1). Consistent with our flow cytometry data (16), we observed increased expression of GZA, *IL2RA*, and *IFN $\gamma$*  in GZB+ versus GZB– CD4 T cells, as well as *NKG7*, a protein reported as involved in CD4 CTL function (27). Other up-regulated genes were linked to cytoskeleton remodeling, DNA binding, glycolysis, and nucleotide metabolism (Table S1). Importantly, three genes in the TNF receptor superfamily (TNFRSF) were enriched in gut GZB+CD4 T cells: *TNFRSF18* (*GITR*), *TNFRSF4* (*OX40*), and *TNFRSF1B* (*CD120b/TNFR2*) (Fig. 4C, Arrows). These three factors can promote T cell division and survival in addition to enhancing memory development and cytokine production (Table S1) (28–31). *OX40* is an upstream regulator of the antiapoptotic protein *BIRC5*, which was reported to promote the survival of HIV-1-infected blood CD4+ T cells (32).

To confirm the expression of these cell surface TNFRSF members at the protein level, LPMCs ( $n = 4$  donors) were cultured with *E. coli* lysate for 48 h and then stained for flow cytometry (Fig. S3A). GZB expression, as expected, increased with *E. coli* lysate stimulation (Fig. 4D and F). Confirming the scRNAseq data, gut GZB+ CD4 T cells had higher frequencies of *CD120b*, *GITR*, and *OX40* than GZB– CD4 T cells (Fig. 4E). There was also a significant increase in the frequency of double and triple-positive CD4 T cells in GZB+ versus GZB– fractions (Fig. S3B). We next evaluated

whether the expression of these TNFRSF members was sustained in culture. At 4 days post-*E. coli* lysate stimulation, *CD120b* and *GITR*, but not *OX40*, were still more frequently detected in GZB+ versus GZB– CD4 T cells (Fig. 4G). Thus, *OX40* induction was transient, making this biomarker less ideal for longitudinal assessments of cell survival in the LPAC model. The presence of canonical GZB inhibitor *Serp1b9*, a hypothesized survival mechanism for GZB+ CD4 T cells, was also examined. At 2 and 4 days post-bacterial stimulation, *Serp1b9* expression was barely detected ( $< 0.5\%$ ) in both GZB+ and GZB– CD4 T cells (Fig. S3C). Altogether, our data reveal that in the absence of HIV-1 infection, a significant subset of bacteria-exposed, gut GZB+ CD4 T cells express canonical survival factors linked to tumor necrosis factor receptor (TNFR) signaling.

### CD120b+ GZB+ CD4 T cells are more frequently infected in the LPAC model than CD120b– counterparts

Given that gut GZB+ CD4 T cells harbor more HIV-1 infection (Fig. 1), we hypothesized that GZB+ CD4 T cells expressing TNFRs may be ideal cellular reservoirs for HIV-1 persistence. To test this hypothesis, LPMCs ( $n = 5$  donors) were infected with TF HIV-1 in the presence of *E. coli* lysate. At 4 dpi, HIV-1 infection was assessed in GZB+ CD4 T cells expressing *GITR* or *CD120b* by

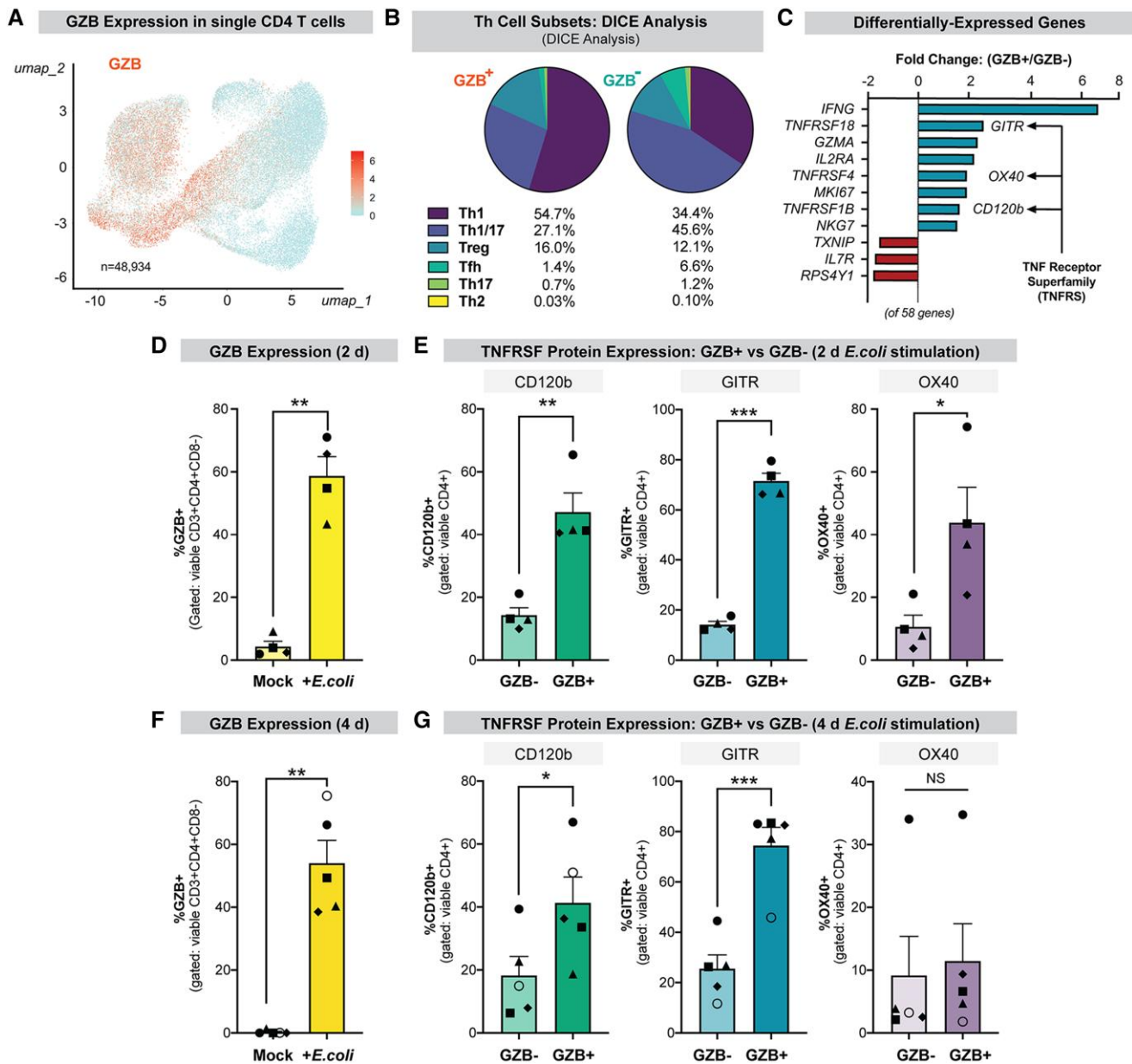


**Fig. 4.** A subset of GZB<sup>+</sup> CD4 T cells express markers associated with cell survival. A) to C) Viable CD4 T cells from LPMC ( $n = 6$  donors) cultured with *E. coli* lysate for 2 days were sorted prior to generation of V3 Chromium Single Cell 3' Transcriptome libraries. Of 48,934 CD4 T cells captured, 15,317 (31%) were GZB<sup>+</sup>. A) Uniform Manifold Approximation and Projection (UMAP) graph of scRNAseq data; each dot represents a single cell; darker dots correspond to GZB<sup>+</sup> CD4 T cells; lighter dots depict GZB<sup>-</sup> CD4 T cells. B) DICE analysis of CD4 T cell subsets in GZB<sup>+</sup> and GZB<sup>-</sup> CD4 T cells. C) Select transcripts up-regulated (blue) and down-regulated (red) in GZB<sup>+</sup> versus GZB<sup>-</sup> CD4 T cells. Arrows indicate TNFRSF genes. The full list of altered 58 genes is given in Table S1. D), F) GZB expression at 2 days ( $n = 4$ ) and 4 days ( $n = 5$ )  $\pm$  *E. coli* lysate stimulation. E), G) TNFRSF protein expression measured by flow cytometry at 2 days ( $n = 4$ ) and 4 days ( $n = 5$ ). For D) to G), differences between groups were evaluated by two-tailed paired t test. Bars represent mean  $\pm$  SEM; \* $P < 0.05$ , \*\* $P < 0.01$ , \*\*\* $P < 0.001$ . ns, not significant.

flow cytometry (Fig. S4). Higher levels of HIV-1 infection (p24<sup>+</sup>) were observed in GZB<sup>+</sup> CD4 T cells expressing CD120b (Fig. 5A), but not GITR (Fig. 5B). CD120b<sup>+</sup> GZB<sup>+</sup> CD4 T cells were also infected at a significantly higher frequency by 6 dpi (Fig. 5C). Thus, in the face of substantial CD4 T cell death, HIV-1 infection is enriched in GZB<sup>+</sup> CD4 T cells expressing CD120b.

To gain more insight on the nature of the CD120b<sup>+</sup> GZB<sup>+</sup> CD4 T cell subpopulation, we revisited our scRNAseq data for molecular features that may distinguish bacteria-induced gut GZB<sup>+</sup> CD4 T cells that express or do not express CD120b (Fig. 5D). Our analysis revealed 519 genes up-regulated > 1.5-fold and 69 genes down-

regulated > 1.5-fold in CD120b<sup>+</sup> versus CD120b<sup>-</sup> GZB<sup>+</sup> CD4 T cells (Fig. S5 and Table S2). Notably, CD120b expression in GZB<sup>+</sup> CD4 T cells was associated with increased expression of antiapoptotic genes (*TWIST1*, *BCL2L15*, *BCL2L1*, *CISH*, and *TNFRSF6B*), as well as genes associated with activation, cytotoxicity, cell adhesion, and both pro- and antiinflammatory cytokine responses (Fig. 5F and Table S2). CD120b<sup>+</sup> GZB<sup>+</sup> CD4 T cells also up-regulated CCR5 and factors that could assist HIV-1 replication such as AP-1 transcription factor subunits (Fig. 5F). By flow cytometry, CD120b<sup>+</sup> GZB<sup>+</sup> CD4 T cells had similar CCR5<sup>+</sup> frequencies compared with CD120b<sup>-</sup> counterparts, but expressed higher CCR5 levels per

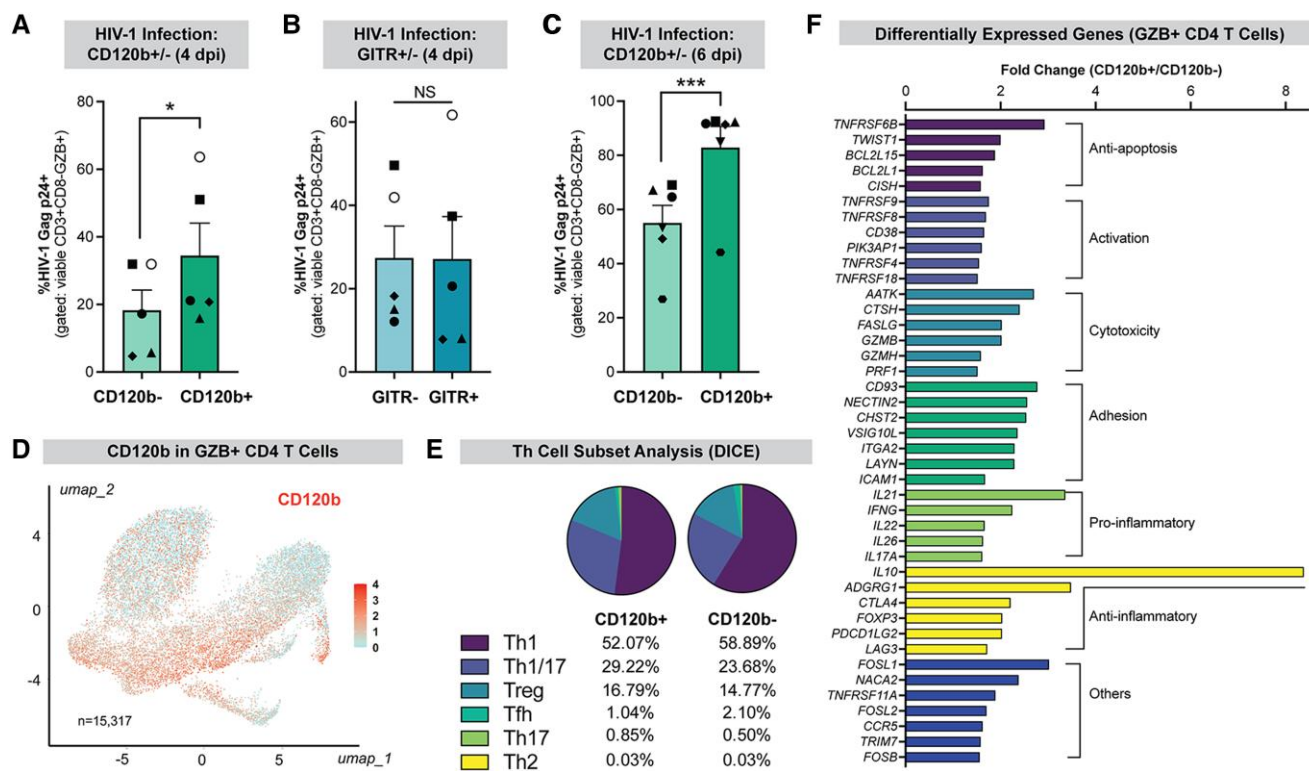


**Fig. 5.** CD120b marks infected GZB+ CD4 T cells in the LPAC model. LPMCs were spinoculated with TF HIV-1 and then cultured for 4 days (A, B) or 6 days (C). HIV-1 infection (in CD3+ CD8- cells) was measured using intracellular p24 flow cytometry. Two-tailed paired t test,  $n = 5$  donors (A, B),  $n = 6$  donors (C). A), C) HIV-1 infection in CD120b  $\pm$  GZB+ CD4 T cells 4 and 6 dpi. B) HIV-1 infection in GITR  $\pm$  GZB+ CD4 T cells. D) to F). Single-cell transcriptome analysis ( $n = 6$  donors; described in Fig. 4A) of 15,317 GZB+ CD4 T cells from LPMC cultured with *E. coli* lysate for 2 days. D) UMAP graph of scRNAseq data; each dot represents a single cell; darker dots correspond to CD120b+ GZB+ CD4 T cells; lighter dots depict CD120b- GZB+ CD4 T cells. E) DICE analysis of CD4 T cell subsets found in CD120b+ versus CD120b- GZB+ CD4 T cells. F) Select transcripts up-regulated in CD120b+ versus CD120b- GZB+ CD4 T cells. The full list of genes, fold-changes, and adjusted *P*-values are given in Table S2. Bars represent mean  $\pm$  SEM. For A to D, \* $P < 0.05$ ; \*\* $P < 0.01$ ; \*\*\* $P < 0.001$ . ns, not significant.

cell (Fig. S6A). A greater fraction of CD120b+ GZB+ CD4 T cells were also activated by 4 days of culture compared with CD120b- counterparts (Fig. S6B).

Skewing of Th cell subsets in CD120b+ versus CD120b- GZB+ CD4 T cells was not apparent by DICE analysis (Fig. 5E), with heterogeneity of Th subsets similar to that of GZB+ cells as a whole. However, the DICE pipeline is based on Th cell subset parameters from the blood, which may limit detection of subtle subset distinctions. CD120b+ GZB+ CD4 T cells expressed higher levels of IL-10, FOXP3 (Fig. 5F), and IKZF2 (Helios; Table S2), suggesting there may be a substantial fraction of CD120b+ GZB+ CD4 T cells that skew toward the Treg subset (33). In fact, 62.5% of CD120b+ GZB+ cells expressed IL-10 (Fig. S7A and Table S3). Interestingly, the majority of these IL-10+ cells co-expressed *IFN- $\gamma$*  and *CTLA-4*, but only a small fraction express “canonical” Treg markers *FOXP3* or *Helios* (Fig. S7B). A substantial fraction (> 50%) of IL-10+ cells expressed survival factors *OX40* and *BCL2L1*, but not *BIRC5* or *CD30* (Fig. S7C). Altogether, these findings reveal that CD120b+ GZB+ CD4 T cells are diverse and express genes associated with cell survival.

### Signaling through CD120b promotes HIV-1 persistence in gut GZB+ CD4 T cells

Our findings above suggest that CD120b+ GZB+ CD4 T cells may have a survival advantage to HIV-1-mediated killing. To test this hypothesis, we analyzed the survival of GZB+ CD120b+ CD4 T cells at 6 dpi ( $n = 6$  donors). At 6 dpi, HIV-1-infected cultures are enriched for CD120b+ GZB+ CD4 T cells relative to mock-infected

cultures (Fig. 6A). Total CD4 T cell depletion was extensive at 6 dpi, as 65% of CD4 T cells died relative to mock-infected controls (Fig. 6B; compared with 43% depletion at 4 dpi, Fig. 3B). There was no significant difference in depletion between GZB+ versus GZB- CD4 T cells at 6 dpi (Fig. 6C). However, GZB+ CD4 T cells expressing CD120b survived at significantly higher levels compared with those not expressing CD120b (Fig. 6D). Co-expression of CD120b provided GZB+ CD4 T cells with a 2.2-fold survival advantage (Fig. 6D). These data suggest that CD120b marks gut GZB+ CD4 T cells that are more likely survive HIV-1 infection in the LPAC model.

The ligand for CD120b, *TNF $\alpha$* , is present in cultures with *E. coli* lysate stimulation (Fig. S8). Thus, signaling through CD120b can potentially occur in the LPAC model. To determine whether the survival advantage of CD120b+ GZB+ CD4 T cells following HIV-1 infection was due to CD120b signaling, we used a CD120b blocking antibody (34), which prevents the interaction between *TNF $\alpha$*  and CD120b. At 0 dpi, LPMCs from five donors were infected with TF HIV-1 by spinoculation, cultured in the presence of *E. coli* lysate, and incubated with either anti-CD120b antibody or a matched isotype control. At 6 dpi, incubation with the isotype control maintained the higher survival rate of GZB+ CD4 T cells expressing CD120b+ versus CD120b- (Fig. 6E, Left). However, this difference was negated by the addition of anti-CD120b (Fig. 6E, Right). These data suggest that the improved survival of GZB+ CD4 T cells expressing CD120b is linked directly to CD120b signaling. Importantly, anti-CD120b treatment reduced the number of HIV-1-infected CD120b+ GZB+ CD4 T cells (Fig. 6F;  $P = 0.055$ ). The

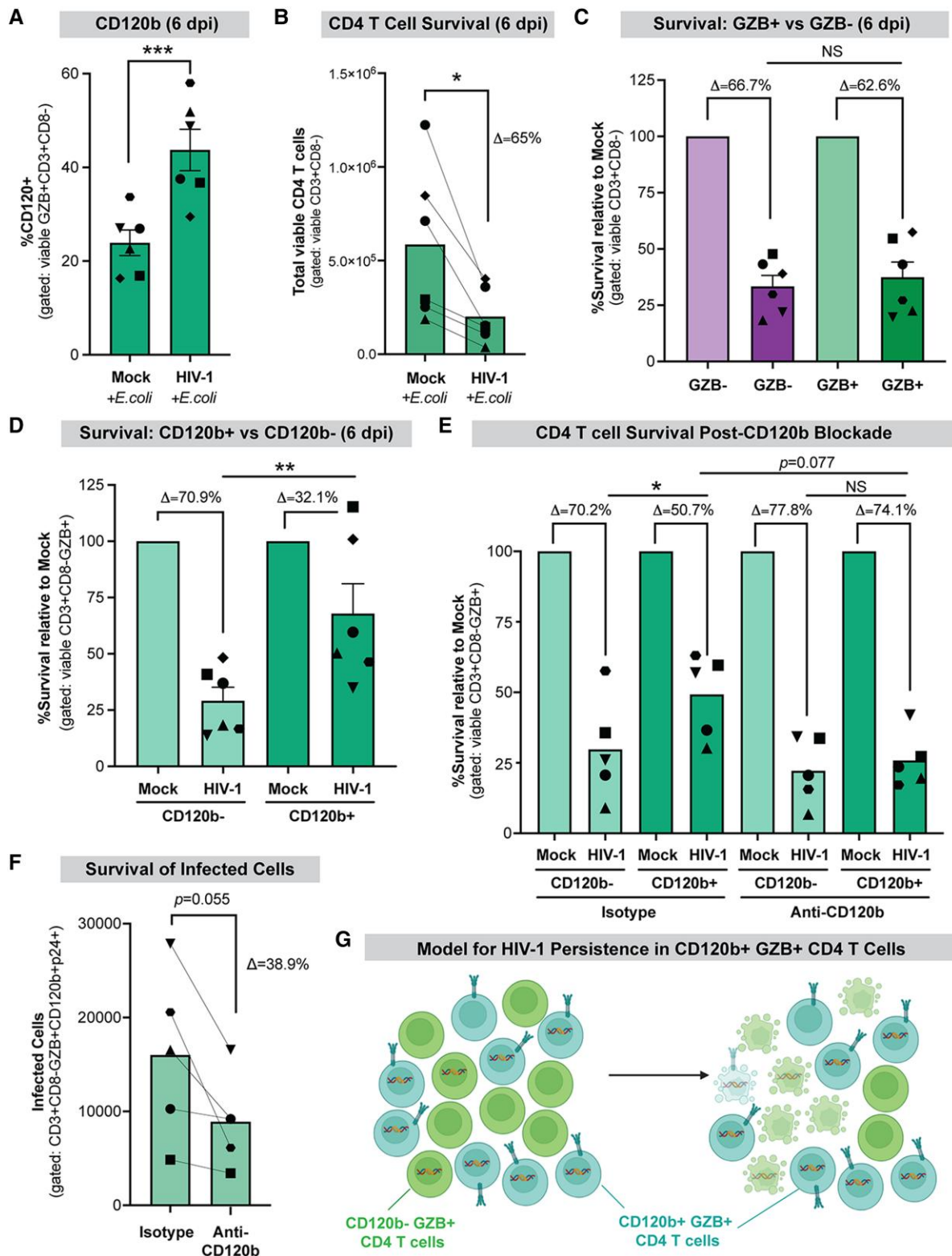


**Fig. 6.** CD120b signaling is associated with GZB+ CD4 T cell survival in the LPAC model. LPMCs were spinoculated with TF HIV-1 and then cultured with *E. coli* lysate for 6 days. A) CD120b expression in gut CD4 T cells in HIV-1- versus mock-infected cultures with *E. coli* ( $n = 6$  donors). B) Difference in absolute CD4 T cell counts between HIV-1-infected and mock ( $n = 6$ ). C) Percent survival of GZB+ versus GZB- CD4 T cells ( $n = 6$  donors). D) Percent survival of CD120b+ versus CD120b- GZB+ CD4 T cells ( $n = 6$  donors). E, F) Effect of CD120b blockade on CD4 T cell survival following HIV-1 infection. LPMCs were incubated with anti-CD120b ( $\alpha$ CD120b) or a matched isotype control at 0 dpi. E) Percent survival of CD120b  $\pm$  GZB+ CD4 T cells. F) Absolute number of infected (p24+) CD120b+ GZB+ CD4 T cells with or without  $\alpha$ CD120b treatment. For C, D, and F, the percent survival was calculated relative to mock (100%) for each donor;  $\Delta$  corresponds to the mean CD4 T cell depletion relative to mock. Group differences in A and B were evaluated by two-tailed paired t test; those in C to E were evaluated using RM one-way ANOVA with Sidak's multiple comparisons test. Bars represent mean ( $\pm$  SEM); \* $P < 0.05$ ; \*\* $P < 0.01$ ; \*\*\* $P < 0.001$ . ns, not significant. G) Model of HIV-1 persistence in CD120b+ GZB+ CD4 T cells (Biorender.com). Cells with a receptor tag represent CD120b+ GZB+ CD4 T cells which have a survival advantage over CD120b- cells. Moreover, CD120b+ cells are more likely to be infected (integrated provirus).



total number of infected CD4 T cells was reduced by anti-CD120b treatment in 4 of 5 LPMC donors, but this did not reach statistical significance (Fig. S9A;  $P=0.10$ ). Anti-CD120b treatment had minimal or no effects on the numbers of HIV-1-infected CD120b<sup>-</sup> GZB<sup>+</sup> CD4 T cells, HIV-1-infected GZB<sup>-</sup> CD4 T cells, HIV-1-uninfected/bystander CD4 T cells, and HIV-1-uninfected/bystander CD120b<sup>+</sup> GZB<sup>+</sup> CD4 T cells (Fig. S9B–E). Altogether, these data implicate CD120b signaling as a mechanism for HIV-1 persistence in gut GZB<sup>+</sup> CD4 T cells (Fig. 6G).

## Discussion

The GI tract is a critical tissue compartment for early HIV-1 pathogenesis, but our understanding of how and why gut CD4 T cells are highly susceptible to HIV-1 mediated death remains incomplete. Prior explanations such as higher CCR5 expression (35, 36), higher baseline CD4 T cell activation (37), alterations in mucosal homing (38), and a favorable proinflammatory microenvironment for HIV-1 replication (39) are all likely involved. However, connecting these observations to molecular features of HIV-1-mediated CD4 T cell death that are unique to the gut versus lymphoid and systemic compartments has remained elusive. Building on extensive data that early HIV-1 infection in the gut is associated with microbial translocation, we discovered that CD4 T cells from the gut, but not the tonsil or blood, readily up-regulate a canonical mediator of cellular cytotoxicity, GZB, following exposure to diverse enteric bacteria (16, 17). Here, we provide evidence using the LPAC model that CD4 T cell-intrinsic GZB significantly contributes to HIV-1-mediated CD4 T cell death. Our finding introduces a novel and unexpected molecular player that could be relevant to prior reports that implicated apoptosis as an important mechanism for HIV-1-mediated CD4 T cell depletion in the GI tract *in vivo* (36, 40, 41).

The underlying molecular mechanism(s) for how GZB promotes HIV-1-mediated gut CD4 T cell death remains to be determined. CD4 CTLs are known to mediate some of their cytotoxic activities through degranulation-dependent mechanisms, similar to cytotoxic CD8 T and NK cell effectors (20). A subset of GZB<sup>+</sup> CD4 T cells in the LPAC model co-express perforin and CD107a, indicating that these cells may kill target cells via canonical CTL degranulation (16). Moreover, we found that gut GZB<sup>+</sup> CD4 T cells also express NKG7, a recently defined marker of CD4 CTL degranulation (27). In the LPAC model with bacterial exposure, HIV-1 killed both virus-infected and bystander (uninfected and abortively infected) CD4 T cells to similar extents, but HIV-1-infected CD4 T cells were more apoptotic. A protease inhibitor known to protect cells from GZB-mediated cytotoxicity, SerpinB9 (42), was barely detected in gut CD4 T cells. Our findings suggest that GZB induction may stimulate “suicide” in HIV-1-infected cells, perhaps in conjunction with viral proteins that promote apoptosis such as Vpr (43). Honing the specific downstream GZB effectors responsible could be challenging. Proteomic studies revealed that over 300 proteins can be targeted by GZB (44). Follow-up work to link GZB targets to TRAIL (45) and Fas/FasL (46) could potentially synthesize the network of reported apoptotic pathways that may contribute to HIV-1-mediated CD4 T cell depletion.

CD4 CTLs can kill target cells via the immunological synapse, providing a potential mechanism for how GZB<sup>+</sup> CD4 T cells can kill bystander CD4 T cells expressing MHC Class II (MHC-II). However, the LPMC donors used in this study were not from PWH, so it is unlikely that the CD4 CTLs we studied were HIV-1-specific. Thus, our model is more relevant to early mucosal

pathogenesis events prior to the induction of HIV-1-specific adaptive immunity. The molecular features of gut CD4 T cells that readily respond to bacteria by up-regulating GZB remain unknown. MHC-II blockade partially inhibited GZB induction in gut CD4 T cells by bacteria (16), suggesting that some (but not all) GZB<sup>+</sup> CD4 T cells may be presenting bacteria-specific ligands (16). The nature of non-MHC-II restricted, bacteria-reactive gut CD4 T cells remains unclear. Interestingly, a large fraction of GZB<sup>+</sup> CD4 T cells do not express perforin (16). Thus, MHC-II- and/or degranulation-independent pathways may also be relevant for how GZB facilitates killing of bystander CD4 T cells. Interestingly, secreted GZB could promote cell death in a perforin-independent manner (47), and CD4 CTLs secrete GZB at a higher level than CD8 CTL (48). Secreted GZB may activate IL-1 $\alpha$  and IL-18 (49, 50), both of which were associated with caspase-1-mediated pyroptosis (51, 52). Pyroptosis was inferred in the LPAC model in the absence of bacterial exposure (14), and caspase-1 activity in colon CD4<sup>+</sup> T cells was detected by 10 days post-infection in simian immunodeficiency virus (SIV)-infected rhesus macaques (53). Further studies would be required to determine the kinetics of GZB induction in human gut CD4<sup>+</sup> T cells during the course of HIV-1 infection in the context of microbial translocation. Altogether, we speculate that GZB could enhance HIV-1-mediated killing of gut CD4 T cells in a multipronged manner. Co-cultures of infected and labeled bystander cells using physical barriers (transwells), pharmacologic inhibitors (anti-retroviral drugs, blockers of cell-signaling), and defined HIV-1 mutants should provide deeper insights on how GZB promotes HIV-1-mediated killing of infected and bystander gut CD4 T cells in the context of bacterial exposure. Of note, extracellular GZB could degrade tight junctional proteins in epithelium and enhance Lipopolysaccharide (LPS)-induced inflammatory cytokine production by antigen-presenting cells (54, 55). Thus, extracellular GZB from microbe-exposed CD4 T cells may also exacerbate microbial translocation and HIV-1-associated mucosal and systemic inflammation.

The latent HIV-1 reservoir persists lifelong despite effective ART and is considered a major barrier to achieving an effective cure (21). This reservoir is established during acute viremia, persists under long-term ART, and is enriched in CD4 CTLs that may be undergoing clonal expansion (22, 56, 57). To date, the source of blood CD4 CTLs harboring persistent HIV-1 remains unknown. GZB<sup>+</sup> CD4 T cells are found at high frequencies during chronic HIV-1 infection in the GI tract (16), GZB is highly induced in gut (but not blood) CD4 T cells following bacterial stimulation *ex vivo* (16), and gut tissue homing and trafficking are disrupted and irregular in PWH (38). Thus, it is possible that the HIV-1 RNA<sup>+</sup> CD4 CTLs identified in peripheral blood of PWH under ART may be in the process of trafficking to or from the gut. Notably, the gut itself may be an important tissue compartment for HIV-1 persistence, as a subset of rebound HIV-1 strains could be traced to the gut (58), and replication-competent HIV-1 has been recovered from PWH under ART (59). However, to our knowledge, the basic mechanisms driving HIV-1 persistence in primary gut CD4 T cells have yet to be investigated in detail.

Building on the theory that the gut HIV-1 reservoir is linked to GZB<sup>+</sup> CD4 T cells that survive HIV-1-mediated CD4 T cell depletion, we utilized single-cell transcriptomics and *in vitro* infection assays and found that a subset expressing CD120b/TNFR2 have a significant survival advantage following HIV-1 infection. Notably, these surviving CD120b<sup>+</sup> GZB<sup>+</sup> CD4 T cells exhibited up to 80% infection rates in the background of high levels of CD4 T cell death. This raises the possibility that viral factors may also contribute to

survival; for example, HIV-1 Nef was reported to exhibit antiapoptotic properties (60). Importantly, blockade experiments suggest that CD120b signaling is directly involved in GZB+ CD4 T cell survival. However, the downstream effectors remain to be determined. In contrast to the canonical TNF $\alpha$  receptor, TNFR1, CD120b lacks a death domain and is known to interact with membrane TNF $\alpha$  to trigger an antiapoptotic and proliferative program involving cIAP1/2 (28). Subsequent activation of the canonical and noncanonical NF- $\kappa$ B pathways results in enhanced IL-2 production, particularly in Tregs (61). Thus, it is feasible that CD120b-mediated induction of IL-2 may be a mechanism that reinforces the survival of GZB+ CD4 T cells. In the LPAC model, bacteria-mediated enhancement of HIV-1-mediated CD4 T cell death is mirrored in Th1 and Th1/17 cells, but a subpopulation of CD4 T cells that were “double-negative” for IFN $\gamma$  and/or IL-17 survive (14). We speculate that the surviving CD4 T cells in the LPAC model are primarily Tregs, but this subset is difficult to study due to the plasticity of canonical markers such as FoxP3 and IL-10 (33). In fact, a FoxP3<sup>-</sup> Treg subset, Tr1, may be involved in maintaining intestinal tolerance (33). In rhesus macaques, IL-10 was linked to SIV persistence during ART in lymph nodes (62). A more detailed dissection of diverse gut Treg subsets in the context of CD120b signaling during the course of HIV-1 infection in the LPAC model would be required to evaluate the contribution of Tregs to GZB+ CD4 T cell survival.

Immunomodulatory therapies targeting TNFR2/CD120b signaling have recently shown promise in oncology (63) and may be repurposed to sensitize HIV-1-infected, CD120b+ gut CD4 T cells to death. However, other antiapoptotic factors in reservoir cells may be conferring a survival advantage (22, 32, 64). In the LPAC model, CD120b+ GZB+ CD4 T cells were also enriched for OX40 and BCL-2-like proteins 1 and 15, but not SerpinB9. HIV-1 reservoir cells have been observed to be resistant to CD8 CTL cell killing (65). Apoptosis-resistant, HIV-1-infected gut CD4 T cells may use similar mechanisms to escape both HIV-1-mediated death and CD8 T cell killing. TNFRSF members, OX40 and CD30, were previously shown to be elevated among HIV-1+ CD4 T cells of PWH (32, 66), and our data show that these markers were also up-regulated gut GZB+ CD4 T cells. HIV-1 cure research may need to account for multiple antiapoptotic mechanisms to sensitize HIV-1 reservoir cells to death.

In conclusion, our findings reveal that bacterial induction of GZB in gut CD4 T cells contributes to HIV-1-mediated CD4 T cell death. A subpopulation of GZB+ CD4 T cells harboring HIV-1 survive, possibly due to antiapoptotic survival mechanisms linked to up-regulated CD120b and TNF signaling in GZB+ CD4 T cells. These findings raise novel insights that may be relevant for HIV-1 pathogenesis and persistence in the gut.

## Methods

### Collection and isolation of human LPMC for in vitro studies

Jejunum samples ( $n=26$  donors) were acquired from patients undergoing elective abdominal surgery ( $n=10$ ) or collected in the process of organ donation ( $n=16$ ) and designated as discarded tissue from macroscopically normal sites. Samples were excluded from the study if patient had a history of inflammatory bowel disease, HIV-1 infection, immunosuppressive drug treatment, or recent chemotherapy (within 8 weeks). LPMCs were isolated from tissue samples in a three-step process to remove mucus and epithelial cells, followed by collagenase digestion to release LPMC as

previously described (13). After processing, LPMCs were cryopreserved in liquid nitrogen. Protected patient information was de-identified prior to data or tissue sharing with laboratory investigators. The Colorado Institutional Review Board (COMIRB) at CU-AMC reviewed the use of LPMC for research (protocol 19-0083) and was deemed Not Human Subject Research as defined by their policies and in accordance with Office of Human Research Protections and U.S. Food and Drug Administration regulations. Each patient tissue sample was considered a single sample. A minimum of four different patient samples were used for each assay.

### Cell culture and in vitro stimulation of LPMC with bacterial lysate

LPMCs were thawed from cryopreservation and cultured in 48-well plate at  $1.0 \times 10^6$  cells/ml in complete Roswell Park Memorial Institute medium (cRPMI): RPMI with 10% human AB serum (Gemini Bioproducts), 1% penicillin/streptomycin/glutamine (Life Technologies), and 500  $\mu$ g/ml Zosyn (piperacillin and tazobactam; Wyeth, Madison, NY, USA) at 37 °C, 5% CO<sub>2</sub> for 2–6 days. Cell cultures were stimulated with commensal *E. coli* (ATCC 25922) lysate from expanded bacteria in appropriate aerobic media as previously detailed (19, 67). Bacterial lysate was prepared from whole-cell bacterial stocks via bead beating and heating. Protein concentration of bacterial lysate was determined by Pierce BCA assay (Thermo-fisher Scientific) as previously described (68). Bacterial lysates were added to the cultures at 10  $\mu$ g/ml.

### Inhibitor treatments in LPMC culture

For GZB inhibition, LPMCs were cultured in the presence or absence of cell-permeable irreversible GZB inhibitor Z-AAD-CMK (Enzo Life Sciences) added once at 250  $\mu$ M with matched sterile H<sub>2</sub>O added to corresponding control conditions. For CD120b/TNFR2 blockade, LPMCs were cultured in the presence of CD120b blocking antibodies (Biolegend) or matched Rat IgG2a isotype control (Biolegend) at 10  $\mu$ g/ml. LPMCs were cultured at 37 °C, 5% CO<sub>2</sub> for 4 or 6 days.

### Viral plasmid stock HIV-1 production and titration

An infectious molecular clone of TF HIV-1 CH040.c (GenBank #JN944939.1) (24) (referred here as CH040) plasmid was prepared using Stbl3 cells (Invitrogen, Carlsbad, CA, USA) and used to produce viral stocks by transfection in 293T cells as previously described (13). Virus stocks were titered using both HIV-1 Gag p24 ELISA kit (Perkin Elmer, Waltham, MA, USA) and TZM-bl infectious virus assay (13). Briefly, TZM-bl reporter cells (NIH AIDS Reagent Program #8129) were plated in 96-well plate; HIV-1 stock virus was added in 5-fold dilutions, mixed, and incubated for 48 h at 37 °C, 5% CO<sub>2</sub>. After 48 h, culture cells were lysed with BriteLite luciferase reagent (Perkin Elmer), and Relative Light Units of luminescence were determined by VictorX5 plate reader (Perkin Elmer).

### HIV-1 infection of LPMCs

LPMCs were thawed using standard protocol detailed previously (13) and resuspended in cRPMI with 10% human AB serum (Gemini Bioproducts), 1% penicillin/streptomycin/glutamine (Life Technologies), and 500  $\mu$ g/ml Zosyn (piperacillin and tazobactam; Wyeth). 500 ng p24 of TF CH040 HIV-1 was spinoculated into  $2.5 \times 10^6$  LPMC. LPMCs were mock infected in parallel. Spinoculation infections were performed at  $1,500 \times g$  for 2 h at

room temperature. After 2 h, supernatant containing free virus was discarded and the LPMCs were washed with phosphate buffered saline (PBS). LPMCs were then resuspended at  $10^6$  LPMCs/ml in cRPMI and plated into 48-well culture plate.

### Quantification of CD4 T cell depletion

After LPMCs were infected as described above ("HIV-1 infection of LPMC"), CD4 T cell depletion was quantified as the difference in the number of viable CD4 (CD3+ CD8-) T cells matched CH040 and mock-infected conditions. The ratio of live mock-infected cells to live CH040 viable T cells is reported as percentage of T cells depleted from the HIV-1-infected wells as previously described (13).

### Gut CD4 T cell magnetic and fluorescent cell isolation for single-cell capture

Total LPMCs were cultured at  $10^6$  cells/ml in the presence of *E. coli* lysate (10  $\mu$ g/ml) at 37°C, 5% CO<sub>2</sub> for 2 days before collection for sorting and single-cell capture. After culture, CD4 T cells were isolated from total LPMC by negative selection (EasySep Human CD4 T cell isolation kit; Stem Cell Technologies) according to the manufacturer's instructions. After magnetic separation, the purified CD4 T cells were further isolated by fluorescence cell sorting. Using standard protocols detailed in flow cytometry staining section, CD4 T cells were stained for viability and surface markers CD45RO, CD3, CD4, and CD8. Flow sorting for viable, CD45RO+, CD3+, CD4, and CD8- cells was completed on the AstriosEQ (Beckman Coulter) for an average enrichment of viable gut CD4 T cells to 99.5%  $\pm$  0.22% ( $n = 6$  donors).

### Single-cell capture, library preparation, and sequencing

The Chromium Single Cell 3' Library and Gel Bead kit v3 (10 $\times$  Genomics) was used to capture, label, and generate transcriptome libraries of individual cells following the manufacturer's instructions. Briefly, the single-cell suspension, RT-PCR master mix, gel beads, and partitioning oil were loaded into a Single Cell A Chip 10 $\times$  Genomics chip, placed into the Chromium Controller, and the Chromium Single Cell A program was run to generate Gel Bead-in-Emulsion (GEM) that contain cell lysates, RT-PCR enzymes, and primers for sequencing, barcoding, and poly-dT sequences. GEMs were transferred to PCR tubes, and RT-PCR was used to generate barcoded single cell-identified cDNA. Barcoded cDNA was used to make sequencing libraries for sequencing analysis. Sequencing was performed on a NovaSeq6000 (Illumina) using paired end 150 cycle $\times$ 150 reads. Cell capture, library preparation, and sequencing were performed by the Genomics and Microarray Core at the University of Colorado Anschutz Medical Campus.

### Analysis of scRNAseq data

scRNAseq data were processed using R and the R package Seurat (version 4.0.3 and version 3.2.3, respectively) (69). The first round of filtering removed cells that had <250 genes and genes that were in <100 cells. In the second round of filtering, cells with a very small library size (<500) or overly high (>7,500) or a high mitochondrial genome transcript ratio (>10%) were removed. Genes were retained if they were detected in >5 cells. Global-scaling normalization was performed using the LogNormalize method and a linear transformation. Dimensionality was determined based on the elbow of a scree plot. Clustering was performed using a graph-based method. First, K-Nearest Neighbor (KNN) graphs based on

the Euclidean distance in principal component analysis (PCA) space was constructed, and then, the edge weights were refined between any two cells based on the shared overlap in their local neighborhoods (Jaccard similarity). The cells are clustered using modularity optimization techniques with the Louvain algorithm.

### Statistical analysis for scRNAseq

Genes were included if the mean gene expression was above 0.1. GZB+ cells were defined as cells that had an expression of GZB above 1 and GZB-negative cells had no GZB expression. A likelihood ratio test was used to determine whether the presence or absence of a gene (other than GZB) in the cell significantly improves the model fit. The full model is a logistic model for the odds of GZB expression with a random intercept for donor and whether the gene is present or absent in the cell. The reduced model did not include whether gene was present or absent. To correct for multiple testing, the Benjamini and Hochberg false discovery rate (FDR) was used (70). Significance was set at and FDR < 0.01. Fold-change of gene expression between GZB+ and GZB- cells was calculated with the normalized gene expression. Automated cell type annotation was performed using the R package singleR, which compares the similarity between query cells and the representative gene expression profile per cell type based on a reference database. In this case, we used the Database of Immune Cell Expression, Expression quantitative trait loci and Epigenomics (DICE) (26) to determine the T cell subsets.

### Flow cytometry staining, acquisition, and analysis

Standard flow cytometry staining protocols were used to stain for viability, cell surface markers (CD3, CD4, CD8, CD45RO, CD120b, GITR, OX40, CD38, HLA-DR, and CCR5), and intracellular expression (GZB, p24, perforin) after Medium A Fixation and Medium B Permeabilization buffer (Life Technologies). Fluorochrome-matched isotype controls were used to establish gates for CD120b, GITR, OX40, CD38, HLA-DR, and CCR5 surface expression and intracellular expression of GZB and perforin. All antibodies and dyes used are included in antibodies for flow cytometry cell culture section of methods. Flow cytometry data were collected on LSRII flow cytometer (BD Biosciences) with routine quality control by Cytometry Setup and Tracking feature within BD FACSDiva software version 6.1.2 (BD Biosciences). Flow cytometry analysis was performed using Flowjo v10.8.1. Gating strategies for representative samples are included in the supplemental figures (Figs. S3 and S4). A table of antibodies utilized is included in the supplement (Table S4).

### GZB activity assay

A colorimetric GZB activity assay was completed using AC-IEPD-*p*-nitroanilide (pNA) (Enzo Life Sciences) (71). In a 96-well plate, cell lysates were added to 2 mM AC-IEPD-pNA and incubated for 24 h. After 24 h, the amount of color change due to released pNA by GZB cleavage of full AC-IEPD-pNA substrate was measured by VictorX5 (Perkin Elmer) absorbance at 405 nm. GZB activity in lysed LPMC was determined based on a standard curve generated using recombinant GZB of known concentration. In two samples treated with GZB inhibitor Z-AAD-CMK, inclusion of the GZB inhibitor in LPMC cultures reduced GZB activity relative to no inhibitor by <15%, and these assays were excluded from further analyses.

## Data statistics and reproducibility

Statistical analysis and data visualization were completed using GraphPad Prism v8.4.2 for windows (GraphPad Software, San Diego, CA, USA). Two-tailed paired t tests and simple and repeated measures ANOVA test with Sidak test for multiple comparisons were utilized as indicated in the figure legends. Data reproducibility in the LPAC model was addressed using biological replicates. Each patient tissue was considered a single sample, and the specific number of donors used in each assay is detailed in figure legends. Statistical analysis for next-generation sequencing data is noted under “Statistical Analysis for scRNAseq.”

## Acknowledgments

The authors thank Jill Slansky, Linda van Dyk, J. David Beckham, and Thomas Morrison for helpful discussions, Christine Purba for assistance with pilot LPMC infections, Martin McCarter and the Pathology Shared Resource Biorepository Core Facility (RRID: SCR\_021989) for access to gut biopsies, Dmitry Baturin and Alistaire Acosta of the Flow Cytometry Shared Resource (P30CA046934) for cell sorting assistance, and Bifeng Gao and Okyong Cho of the Genomics Shared Resource (RRID: SCR\_021984) for assistance with next-generation sequencing. Special thanks to Christina Oschenbauer for providing the CH40.c infectious molecular clone and John Kappes for the TZM-bl cells.

## Supplementary Material

[Supplementary material](#) is available at PNAS Nexus online.

## Funding

This work was supported by the National Institutes of Health (NIH) R01 AI108404 and AI134220 (C.C.W. and M.L.S.), the Colorado Clinical and Translational Sciences Institute NIH UM1 TR004399 and T32 TR004367 (K.L.M.), the NIH Molecular Pathogenesis of Infectious Disease T32 AI052066-19 (K.L.M.), the University of Colorado RNA Bioscience Institute (M.L.S., C.C.W., and K.G.), and the University of Colorado ASPIRE Program (M.L.S., C.C.W., K.K., S.M.D., and K.G.).

## Author Contributions

M.L.S., C.C.W., K.L.M., and S.M.D. designed the study. K.L.M. and M.L.S. prepared the figures and wrote the initial drafts of the manuscript, which were revised by C.C.W. and S.M.D. K.L.M. performed the bulk of experiments in the LPAC model with technical assistance from A.N.T., K.G., and B.S.B. and advice on immunology from S.M.D. and C.C.W. and virology from M.L.S. K.L.M. performed the statistical analyses. K.G., C.W., and K.K. analyzed the scRNAseq data using bioinformatics pipelines and performed the statistical analyses. All authors read and contributed to writing the final version of the manuscript.

## Data Availability

Single-cell RNAseq data were deposited in GEO, under accession number GSE268231. Source files are provided in this link.

## References

- Fahey JL, et al. 1990. The prognostic value of cellular and serologic markers in infection with human immunodeficiency virus type 1. *N Engl J Med.* 322:166–172.
- Brenchley JM, Douek DC. 2008. HIV infection and the gastrointestinal immune system. *Mucosal Immunol.* 1:23–30.
- Doitsh G, et al. 2014. Cell death by pyroptosis drives CD4 T-cell depletion in HIV-1 infection. *Nature.* 505:509–514.
- Miller SM, et al. 2017. Follicular regulatory T cells are highly permissive to R5-tropic HIV-1. *J Virol.* 91:e00430-17.
- Mehandru S, Dandekar S. 2008. Role of the gastrointestinal tract in establishing infection in primates and humans. *Curr Opin HIV AIDS.* 3:22–27.
- Wang Q, et al. 2024. The CARD8 inflammasome dictates HIV/SIV pathogenesis and disease progression. *Cell.* 187:1223–1237.e16.
- Zhang C, et al. 2023. Humanized mice for studies of HIV-1 persistence and elimination. *Pathogens.* 12:879.
- Sender R, Fuchs S, Milo R. 2016. Revised estimates for the number of human and bacteria cells in the body. *PLoS Biol.* 14:e1002533.
- Zevin AS, McKinnon L, Burgener A, Klatt NR. 2016. Microbial translocation and microbiome dysbiosis in HIV-associated immune activation. *Curr Opin HIV AIDS.* 11:182–190.
- Marchetti G, Tincati C, Silvestri G. 2013. Microbial translocation in the pathogenesis of HIV infection and AIDS. *Clin Microbiol Rev.* 26:2–18.
- Deeks SG, Tracy R, Douek DC. 2013. Systemic effects of inflammation on health during chronic HIV infection. *Immunity.* 39:633–645.
- Zicari S, et al. 2019. Immune activation, inflammation, and non-AIDS co-morbidities in HIV-infected patients under long-term ART. *Viruses.* 11:200.
- Dillon SM, Guo K, Castleman MJ, Santiago ML, Wilson CC. 2020. Quantifying HIV-1-mediated gut CD4+ T cell death in the Lamina Propria Aggregate Culture (LPAC) model. *Bio Protoc.* 10:e3486.
- Steele AK, et al. 2014. Microbial exposure alters HIV-1-induced mucosal CD4+ T cell death pathways ex vivo. *Retrovirology.* 11:14.
- Dillon SM, et al. 2012. HIV-1 infection of human intestinal lamina propria CD4+ T cells in vitro is enhanced by exposure to commensal *Escherichia coli*. *J Immunol.* 189:885–896.
- Dillon SM, et al. 2022. Granzyme B(+) CD4 T cells accumulate in the colon during chronic HIV-1 infection. *Gut Microbes.* 14:2045852.
- Yoder AC, et al. 2017. The transcriptome of HIV-1 infected intestinal CD4+ T cells exposed to enteric bacteria. *PLoS Pathog.* 13:e1006226.
- Harper MS, et al. 2015. Interferon-alpha subtypes in an ex vivo model of acute HIV-1 infection: expression, potency and effector mechanisms. *PLoS Pathog.* 11:e1005254.
- Dillon SM, et al. 2016. Enhancement of HIV-1 infection and intestinal CD4+ T cell depletion ex vivo by gut microbes altered during chronic HIV-1 infection. *Retrovirology.* 13:5.
- Chowdhury D, Lieberman J. 2008. Death by a thousand cuts: granzyme pathways of programmed cell death. *Annu Rev Immunol.* 26:389–420.
- Siliciano JD, Siliciano RF. 2022. In vivo dynamics of the latent reservoir for HIV-1: new insights and implications for cure. *Annu Rev Pathol.* 17:271–294.
- Collora JA, et al. 2022. Single-cell multiomics reveals persistence of HIV-1 in expanded cytotoxic T cell clones. *Immunity.* 55:1013–1031.e7.

- 23 Geretz A, et al. 2023. Single-cell transcriptomics identifies prothymosin alpha restriction of HIV-1 in vivo. *Sci Transl Med.* 15: eadg0873.
- 24 Ochsenbauer C, et al. 2012. Generation of transmitted/founder HIV-1 infectious molecular clones and characterization of their replication capacity in CD4 T lymphocytes and monocyte-derived macrophages. *J Virol.* 86:2715–2728.
- 25 Thornberry NA, et al. 1997. A combinatorial approach defines specificities of members of the caspase family and granzyme B. Functional relationships established for key mediators of apoptosis. *J Biol Chem.* 272:17907–17911.
- 26 Schmiedel BJ, et al. 2018. Impact of genetic polymorphisms on human immune cell gene expression. *Cell.* 175:1701–1715.e16.
- 27 Ng SS, et al. 2020. The NK cell granule protein NKG7 regulates cytotoxic granule exocytosis and inflammation. *Nat Immunol.* 21:1205–1218.
- 28 Croft M. 2014. The TNF family in T cell differentiation and function—unanswered questions and future directions. *Semin Immunol.* 26:183–190.
- 29 Brenner D, Blaser H, Mak TW. 2015. Regulation of tumour necrosis factor signalling: live or let die. *Nat Rev Immunol.* 15:362–374.
- 30 Ronchetti S, Nocentini G, Riccardi C, Pandolfi PP. 2002. Role of GITR in activation response of T lymphocytes. *Blood.* 100:350–352.
- 31 Withers DR, et al. 2009. The survival of memory CD4+ T cells within the gut lamina propria requires OX40 and CD30 signals. *J Immunol.* 183:5079–5084.
- 32 Kuo HH, et al. 2018. Anti-apoptotic protein BIRC5 maintains survival of HIV-1-infected CD4(+) T cells. *Immunity.* 48:1183–1194.e5.
- 33 Figliuolo da Paz VR, Jamwal DR, Kiela PR. 2021. Intestinal regulatory T cells. *Adv Exp Med Biol.* 1278:141–190.
- 34 Sheehan KC, et al. 1995. Monoclonal antibodies specific for murine p55 and p75 tumor necrosis factor receptors: identification of a novel in vivo role for p75. *J Exp Med.* 181:607–617.
- 35 Brenchley JM, et al. 2004. CD4+ T cell depletion during all stages of HIV disease occurs predominantly in the gastrointestinal tract. *J Exp Med.* 200:749–759.
- 36 Mehandru S, et al. 2004. Primary HIV-1 infection is associated with preferential depletion of CD4+ T lymphocytes from effector sites in the gastrointestinal tract. *J Exp Med.* 200:761–770.
- 37 Mehandru S, et al. 2007. Mechanisms of gastrointestinal CD4+ T-cell depletion during acute and early human immunodeficiency virus type 1 infection. *J Virol.* 81:599–612.
- 38 Mavigner M, et al. 2012. Altered CD4+ T cell homing to the gut impairs mucosal immune reconstitution in treated HIV-infected individuals. *J Clin Invest.* 122:62–69.
- 39 McGowan I, et al. 2004. Increased HIV-1 mucosal replication is associated with generalized mucosal cytokine activation. *J Acquir Immune Defic Syndr.* 37:1228–1236.
- 40 Li Q, et al. 2005. Peak SIV replication in resting memory CD4+ T cells depletes gut lamina propria CD4+ T cells. *Nature.* 434:1148–1152.
- 41 Mattapallil JJ, et al. 2005. Massive infection and loss of memory CD4+ T cells in multiple tissues during acute SIV infection. *Nature.* 434:1093–1097.
- 42 Hirst CE, et al. 2003. The intracellular granzyme B inhibitor, proteinase inhibitor 9, is up-regulated during accessory cell maturation and effector cell degranulation, and its overexpression enhances CTL potency. *J Immunol.* 170:805–815.
- 43 Vanegas-Torres CA, Schindler M. 2024. HIV-1 Vpr functions in primary CD4(+) T cells. *Viruses.* 16:420.
- 44 Van Damme P, et al. 2009. Analysis of protein processing by N-terminal proteomics reveals novel species-specific substrate determinants of granzyme B orthologs. *Mol Cell Proteomics.* 8: 258–272.
- 45 Herbeuval JP, et al. 2005. Regulation of TNF-related apoptosis-inducing ligand on primary CD4+ T cells by HIV-1: role of type I IFN-producing plasmacytoid dendritic cells. *Proc Natl Acad Sci U S A.* 102:13974–13979.
- 46 Dyrhol-Riise AM, et al. 2001. The Fas/FasL system and T cell apoptosis in HIV-1-infected lymphoid tissue during highly active antiretroviral therapy. *Clin Immunol.* 101:169–179.
- 47 Gondek DC, Lu LF, Quezada SA, Sakaguchi S, Noelle RJ. 2005. Cutting edge: contact-mediated suppression by CD4+ CD25+ regulatory cells involves a granzyme B-dependent, perforin-independent mechanism. *J Immunol.* 174:1783–1786.
- 48 Lin L, et al. 2014. Granzyme B secretion by human memory CD4 T cells is less strictly regulated compared to memory CD8 T cells. *BMC Immunol.* 15:36.
- 49 Omoto Y, et al. 2010. Granzyme B is a novel interleukin-18 converting enzyme. *J Dermatol Sci.* 59:129–135.
- 50 Afonina IS, et al. 2011. Granzyme B-dependent proteolysis acts as a switch to enhance the proinflammatory activity of IL-1alpha. *Mol Cell.* 44:265–278.
- 51 Yu P, et al. 2021. Pyroptosis: mechanisms and diseases. *Signal Transduct Target Ther.* 6:128.
- 52 Aizawa E, et al. 2020. GSDME-dependent incomplete pyroptosis permits selective IL-1alpha release under caspase-1 inhibition. *iScience.* 23:101070.
- 53 He X, et al. 2022. Rapid loss of CD4 T cells by pyroptosis during acute SIV infection in rhesus macaques. *J Virol.* 96:e0080822.
- 54 Matsubara JA, et al. 2020. Retinal distribution and extracellular activity of granzyme B: a serine protease that degrades retinal pigment epithelial tight junctions and extracellular matrix proteins. *Front Immunol.* 11:574.
- 55 Obasanmi G, et al. 2023. Granzyme B contributes to choroidal neovascularization and age-related macular degeneration through proteolysis of thrombospondin-1. *Lab Invest.* 103:100123.
- 56 Maldarelli F, et al. 2014. HIV latency. Specific HIV integration sites are linked to clonal expansion and persistence of infected cells. *Science (New York, N.Y.).* 345:179–183.
- 57 Wagner TA, et al. 2014. HIV latency. Proliferation of cells with HIV integrated into cancer genes contributes to persistent infection. *Science (New York, N.Y.).* 345:570–573.
- 58 Rothenberger MK, et al. 2015. Large number of rebounding/founder HIV variants emerge from multifocal infection in lymphatic tissues after treatment interruption. *Proc Natl Acad Sci U S A.* 112:E1126–E1134.
- 59 Vellas C, et al. 2024. Intact proviruses are enriched in the colon and associated with PD-1(+)/TIGIT(-) mucosal CD4(+) T cells of people with HIV-1 on antiretroviral therapy. *EBioMedicine.* 100: 104954.
- 60 Geleziunas R, Xu W, Takeda K, Ichijo H, Greene WC. 2001. HIV-1 Nef inhibits ASK1-dependent death signalling providing a potential mechanism for protecting the infected host cell. *Nature.* 410: 834–838.
- 61 Yang S, Wang J, Brand DD, Zheng SG. 2018. Role of TNF-TNF receptor 2 signal in regulatory T cells and its therapeutic implications. *Front Immunol.* 9:784.
- 62 Harper J, et al. 2022. Interleukin-10 contributes to reservoir establishment and persistence in SIV-infected macaques treated with antiretroviral therapy. *J Clin Invest.* 132:e155251.
- 63 Medler J, Kucka K, Wajant H. 2022. Tumor necrosis factor receptor 2 (TNFR2): an emerging target in cancer therapy. *Cancers (Basel).* 14:2603.

- 64 Cummins NW, et al. 2017. Maintenance of the HIV reservoir is antagonized by selective BCL2 inhibition. *J Virol.* 91:e00012–e00017.
- 65 Huang SH, et al. 2018. Latent HIV reservoirs exhibit inherent resistance to elimination by CD8+ T cells. *J Clin Invest.* 128:876–889.
- 66 Hogan LE, et al. 2018. Increased HIV-1 transcriptional activity and infectious burden in peripheral blood and gut-associated CD4+ T cells expressing CD30. *PLoS Pathog.* 14:e1006856.
- 67 Castleman MJ, et al. 2019. Commensal and pathogenic bacteria indirectly induce IL-22 but not IFN $\gamma$  production from human colonic ILC3s via multiple mechanisms. *Front Immunol.* 10:649.
- 68 Dillon SM, et al. 2020. Age-related alterations in human gut CD4 T cell phenotype, T helper cell frequencies, and functional responses to enteric bacteria. *J Leukoc Biol.* 107:119–132.
- 69 Stuart T, et al. 2019. Comprehensive integration of single-cell data. *Cell.* 177:1888–1902 e1821.
- 70 Benjamini Y, Hochberg Y. 1995. Controlling the false discovery rate: a practical and powerful approach to multiple testing. *J R Stat Soc Ser B (Methodol).* 57:289–300.
- 71 Hagn M, Sutton VR, Trapani JA. 2014. A colorimetric assay that specifically measures granzyme B proteolytic activity: hydrolysis of Boc-Ala-Ala-Asp-S-Bzl. *J Vis Exp.* (93):e52419.